# Solubilization of green plant thylakoid membranes with n-dodecyl-α,D-maltoside. Implications for the structural organization of the Photosystem II, Photosystem I, ATP synthase and cytochrome b6f complexes

Roon, Henny van; Breemen, Jan F.L. van; Weerd, Frank L. de; Dekker, Jan P.; Boekema, Egbert J.

*Published in:*
Journal of Molecular Biology



*Publication date:*
2000

*Photosynthesis Research* **64:** 155–166, 2000.



*Regular paper*

# Solubilization of green plant thylakoid membranes with *n*-dodecyl-$\alpha$,D-maltoside. Implications for the structural organization of the Photosystem II, Photosystem I, ATP synthase and cytochrome $b_6$ *f* complexes

Henny van Roon[1], Jan F.L. van Breemen[2], Frank L. de Weerd[1], Jan P. Dekker[1,*] & Egbert J. Boekema[2]

[1]*Faculty of Sciences, Division of Physics and Astronomy, Vrije Universiteit, De Boelelaan 1081, 1081 HV Amsterdam, The Netherlands;* [2]*Department of Biophysical Chemistry, Groningen Biomolecular Sciences and Biotechnology Institute, University of Groningen, Nijenborgh 4, 9747 AG Groningen, The Netherlands;* [*]*Author for correspondence (e-mail: dekker@nat.vu.nl; fax: +31-20-4447999)*

Received 2 February 2000; accepted in revised form 13 April 2000

*Key words:* $CF_0F_1$, cytochrome $b_6f$, electron microscopy, grana, Photosystem I, Photosystem II

**Abstract**

A biochemical and structural analysis is presented of fractions that were obtained by a quick and mild solubilization of thylakoid membranes from spinach with the non-ionic detergent *n*-dodecyl-$\alpha$,D-maltoside, followed by a partial purification using gel filtration chromatography. The largest fractions consisted of paired, appressed membrane fragments with an average diameter of about 360 nm and contain Photosystem II (PS II) and its associated light-harvesting antenna (LHC II), but virtually no Photosystem I, ATP synthase and cytochrome $b_6f$ complex. Some of the membranes show a semi-regular ordering of PS II in rows at an average distance of about 26.3 nm, and from a partially disrupted grana membrane fragment we show that the supercomplexes of PS II and LHC II represent the basic structural unit of PS II in the grana membranes. The numbers of free LHC II and PS II core complexes were very high and very low, respectively. The other macromolecular complexes of the thylakoid membrane occurred almost exclusively in dispersed forms. Photosystem I was observed in monomeric or multimeric PS I-200 complexes and there are no indications for free LHC I complexes. An extensive analysis by electron microscopy and image analysis of the $CF_0F_1$ ATP synthase complex suggests locations of the $\delta$ (on top of the $F_1$ headpiece) and $\epsilon$ subunits (in the central stalk) and reveals that in a substantial part of the complexes the $F_1$ headpiece is bended considerably from the central stalk. This kinking is very likely not an artefact of the isolation procedure and may represent the complex in its inactive, oxidized form.

*Abbreviations:* $\alpha$-DM – *n*-dodecyl-$\alpha$,D-maltoside; BBY – PS II membranes prepared according to Berthold, Babcock and Yocum (1981); $\beta$-DM – *n*-dodecyl-$\beta$,D-maltoside; Chl – chlorophyll; LHC I – light-harvesting complex I; LHC II – light-harvesting complex II; MSP – manganese stabilizing protein; PS I – Photosystem I; PS II – Photosystem II

## Introduction

The thylakoid membranes of green plant chloroplasts comprise one of the most complex and dynamic membrane systems in biology (Staehelin and van der Staay 1996). Within a chloroplast, these membranes form a continuous three-dimensional network that consists of two clearly distinct types of membrane domains. One type is formed by cylindrical stacks of appressed thylakoids, known as grana, and the other, the so-called stroma membranes, appear as flattened tubules, interconnecting the grana stacks. The stacking is me-

diated by the presence of divalent cations and leads to a concentration of Photosystem II (PS II) and its associated light-harvesting antenna (LHC II). Photosystem I (PS I) and its associated light-harvesting antenna (LHC I) and the ATP synthase complex are predominantly restricted to the non-stacked areas of the thylakoid membranes, whereas the cytochrome $b_6f$ complex is probably more or less evenly distributed over the stacked and non-stacked parts of the thylakoid membranes.

Within the last decade, impressive progress has been made on the structure and organization of essential parts of the protein complexes involved in the photosynthetic light reactions (see, e.g., Kühlbrandt et al. 1994; Schubert et al. 1997; Rhee et al. 1998). Despite this progress, however, it is still not known how the various proteins in the thylakoid membranes cooperate to convert the light energy so efficiently. This type of knowledge is very important, also because structural rearrangements in the thylakoid membranes form the basis of several regulatory processes of the photosynthetic light reactions (e.g., the state transitions, non-photochemical quenching and the xanthophyll cycle, the extremely rapid turnover of some PS II proteins and the repair mechanisms occurring after photoinhibitory damage).

A large part of our knowledge of the structural organization of the thylakoid membranes has been obtained from freeze-fracture and freeze-etch electron microscopy (Staehelin and van der Staay 1996), which give images with structural detail at about 40–50 Å resolution. Considerably more detail, however, is required to understand the role of the various proteins in the energy flow to the reaction center and in the dynamics related to short-term acclimation processes. In order to get more insight in the structure and dynamics of the thylakoid membrane we recently developed new methods to prepare macromolecular protein associations occurring in these membranes in as-native-as-possible states and analyzed these macromolecules by transmission electron microscopy and image analysis, using negatively stained specimens. We solubilized PS II membrane fragments obtained by Triton X-100 treatment of stacked thylakoids (Berthold et al. 1981) with the very mild detergent *n*-dodecyl-$\alpha$,D-maltoside ($\alpha$-DM) and reduced the amount of detergent and the time of detergent exposure to an absolute minimum to prevent the fragmentation of the fragile macromolecular complexes as much as possible (Boekema et al. 1998, 1999a, b). The results revealed the presence of various types of PS II supercomplexes (dimeric PS II core complexes to which various numbers of trimeric and monomeric LHC II complexes are attached) and megacomplexes (dimeric associations of some of the PS II supercomplexes), as well as a heptameric association of trimeric LHC II, the so-called icosienamer (Dekker et al. 1999).

In this paper we investigate the use of $\alpha$-DM for the solubilization of intact thylakoid membranes and show that under certain conditions this detergent effectively solubilizes the components of the stroma lamellae but leaves the grana membranes relatively intact as paired, appressed membrane fragments. The structural organization of these membrane fragments resembles those prepared with Triton X-100 (Dunahay et al. 1984), although the $\alpha$-DM treatment seems to preserve to a much larger extent a higher order of regularity in the packing of the PS II supercomplexes, which are considered to form the basic structural unit of PS II in the stacked parts of the thylakoid membranes (see, e.g., Boekema et al. 1999a, b; Nield et al. 2000). The most important advantage of the use of $\alpha$-DM is the intactness of the solubilized fractions, which will allow an extensive characterization of the components of the stromal membranes, such as the native PS I complex and $CF_0F_1$ ATP synthase complex. Some recent results on the structure of the latter complex will be discussed in more detail.

## Materials and methods

Freshly prepared thylakoid membranes at a chlorophyll concentration of 1.4 mg/ml were suspended at 4 °C in a buffer containing 20 mM BisTris (pH 6.5) and 5 mM $MgCl_2$, solubilized with *n*-dodecyl-$\alpha$,D-maltoside ($\alpha$-DM, final concentration 1.2%) during 1 min and centrifuged for 3 min at 9000 rpm in an Eppendorf table centrifuge, after which the supernatant was pushed through a 0.45 $\mu$m filter to remove large fragments. The solubilized fractions were subjected to gel filtration chromatography as described by Eijckelhoff et al. (1996) using a Superdex 200 HR 10/30 column (Pharmacia) with 20 mM BisTris (pH 6.5), 5 mM $MgCl_2$ and 0.03% $\alpha$-DM as mobile phase and a flow rate of 25 ml/h. The chromatography was performed at room temperature, while for detection a Waters 990 diode array detector was used. After the appearance of the first green material at 16.3 min after supplying the solubilized thylakoids to the gel filtration column, 13 fractions of 0.6 ml each were pooled, kept at 4 °C and further analyzed within one hour. The

particles were kept in darkness during the complete isolation procedure. For the low temperature fluorescence measurements the fractions were diluted in the above-mentioned BisTris/$MgCl_2$/$\alpha$-DM buffer + 75% (v/v) glycerol to an optical density at 679 nm of about 0.1 $cm^{-1}$.

Chlorophyll *a* and *b* contents were measured in 80% acetone using the extinction coefficients reported by Porra et al. (1989). Absorption spectra were recorded at room temperature with a Lambda 40 spectrophotometer (Perkin Elmer). Contents of cytochrome *f* were evaluated from the peak at 555 nm in the ascorbate-reduced minus ferricyanide-oxidized difference spectrum (corrected for baseline effects). Fluorescence emission spectra were measured with a 1/2 m imaging spectrograph (Chromex 500IS) and a CCD camera (Chromex Chromcam I) with a spectral resolution of 0.5 nm. Broadband excitation was applied using a tungsten halogen lamp (Oriel) and a bandpass filter transmitting at 420 nm (bandwidth ± 20 nm). The samples were contained in a helium-bath cryostat (Utreks, 4K). SDS-PAGE was performed on a 12% acrylamide gel according to Schägger and von Jagow (1987).

Transmission electron microscopy was performed with a Philips cm10 electron microscope at 52,000 × magnification. Negatively stained specimens were prepared with a 2% solution of uranyl acetate on glow-discharged carbon-coated copper grids as in Boekema et al. (1999a). Projections were extracted for image analysis with IMAGIC software (Harauz et al. 1988) following alignment procedures and treatment by multivariate statistical analysis (Van Heel and Frank 1981) and classification (Van Heel 1989) as described previously (Boekema et al. 1999a) on a Silicon graphics octane computer.

## Gel filtration chromatography

Incubation of spinach thylakoid membranes at a chlorophyll concentration of 1.4 mg/ml with 1.2% $\alpha$-DM usually resulted in a very quick and almost complete 'solubilization' of the membranes, even at 4 °C. We note that the term 'solubilization' is defined here rather arbitrarily as the property to stay in the supernatant after a 3 min centrifugation at 9000 rpm in a table centrifuge (see 'Materials and methods'). This effectively means that a complete solubilization to individual membrane protein complexes is not required for this procedure and that 'non-solubilized' membrane fragments are also included, as long as they are not much larger than about 0.45 $\mu$m (because the 'solubilized' material was passed through a 0.45 $\mu$m filter before it was subjected to the gel filtration chromatography). Figure 1 (full line) shows a typical chromatogram, recorded at 400 nm. The suspension usually fractionates into six main fractions peaking at about 18, 20, 23, 28, 31 and 34 mins, which appear maximally in fractions 1, 3, 5, 9, 11 and 13, respectively. First indications of the identity of the various fractions were obtained by the simultaneously recorded ratios of the absorbances at 480 and 410 nm (dashed line) and at 700 and 670 nm (dotted line). The $A_{480}/A_{410}$ ratio roughly monitors the ratio of chlorophyll *b* and chlorophyll *a* (and to some extent also the carotenoid content), whereas the $A_{700}/A_{670}$ ratio monitors the relative content of long-wavelength absorbing chlorophylls, which are predominantly present in PS I. Both ratios vary quite considerably during chromatography (Figure 1) and indicate that fraction 1 is enriched in PS II (low $A_{700}/A_{670}$ ratio) and LHC II (high $A_{480}/A_{410}$ ratio), fractions 3 and 5 are enriched in PS I (low $A_{480}/A_{410}$ ratio and high $A_{700}/A_{670}$ ratio), fraction 9 consists primarily of trimeric LHC II (high $A_{480}/A_{410}$ ratio), fraction 11 is enriched in mono-

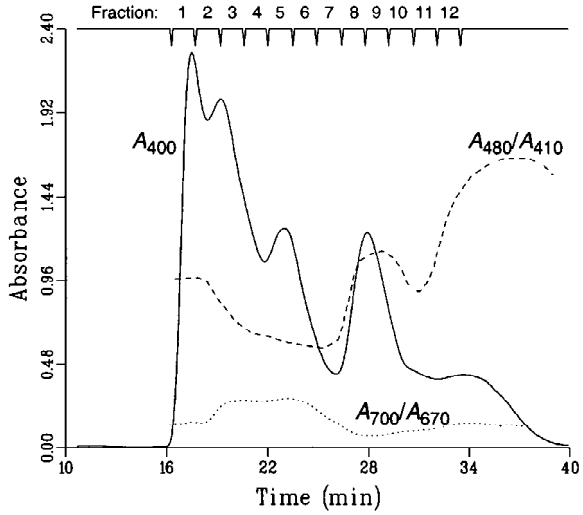


*Figure 1.* FPLC gel filtration chromatogram (full line) recorded at 400 nm of spinach thylakoid membranes solubilized with $\alpha$-DM. The chromatogram is plotted together with the $A_{480}/A_{410}$ ratio (dashed line) and the $A_{700}/A_{670}$ ratio (dotted line) to get information on the relative contents of Chl *b* + carotenoids and the long-wavelength antenna chlorophylls, respectively. The values on the y-axis are the real values of these ratios. The flow rate was 25 ml/h. The upper scale represents the fractions on which the various biochemical and structural studies shown in Figures 2–7 were performed.

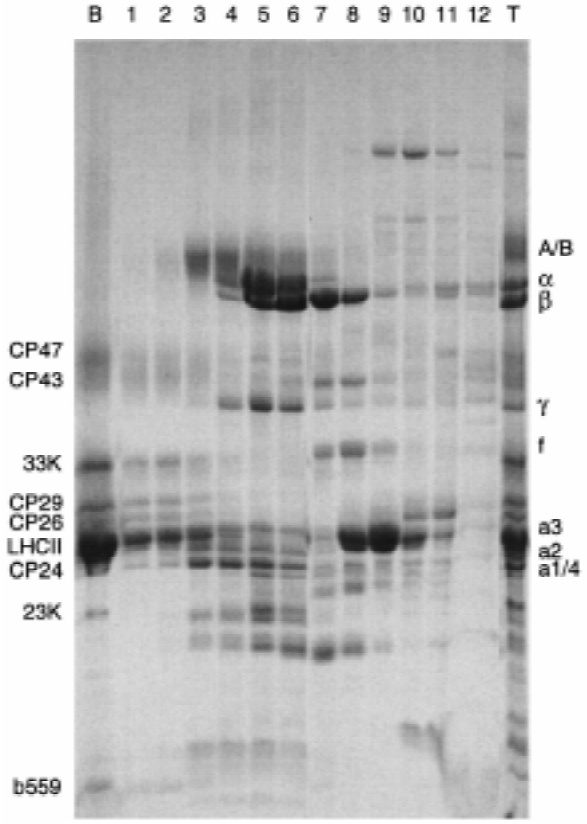


*Figure 2.* Identification of polypeptides in chromatography-purified, $\alpha$-DM-solubilized thylakoid membranes by SDS-PAGE. The lanes designated 'B' and 'T' show the polypeptide composition of BBY and thylakoid membranes, respectively, whereas the lanes designated '1' to '12' show the polypeptide composition of the corresponding fractions from the gel filtration column (Figure 1). The volume of applied sample was the same for fractions 2–12 and two times smaller for fraction 1. The gel was stained with Coomassie Brilliant Blue. On the left side of the gel the positions of the most of the PS II proteins are depicted while on the right side the positions of some of the PS I, ATPase and cytochrome $b_6f$ proteins are shown.

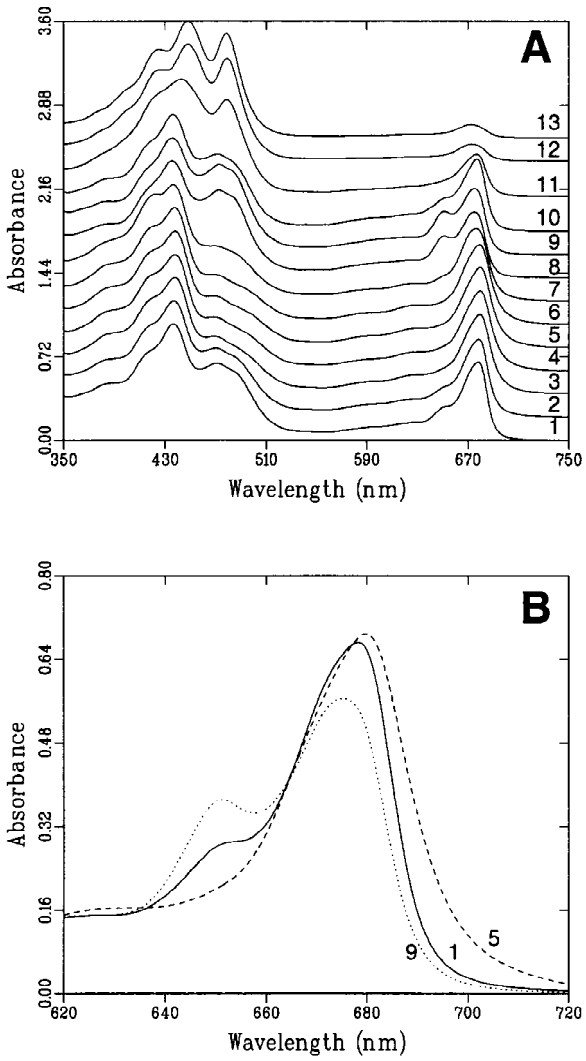


*Figure 3.* Room temperature absorption spectra of fractions 1–13 from the gel filtration chromatography, normalized to 1 at the maximum absorption value. In (A) the fractions 2–13 are shown with an offset to illustrate the differences. In (B) the $Q_y$ absorption regions are shown of fractions 1 (full line), 5 (dashed line) and 9 (dotted line), normalized as in (A) but without the offset.

meric LHC II proteins (a lower $A_{480}/A_{410}$ ratio and a low $A_{700}/A_{670}$ ratio) and fraction 13 is enriched in carotenoids (because of the extremely high $A_{480}/A_{410}$ ratio).

The various fractions have been further analyzed by SDS-PAGE (Figure 2), the ratio of chlorophylls *a* and *b* (Table 1), absorption spectra at room temperature (Figure 3 and Table 1), the content of cytochrome *f* (Table 1), emission spectra at 4 K (Figure 4) and transmission electron microscopy (Figures 5–7). In the following, we discuss the appearance and properties of the various macromolecular assemblies, i.e., PS II, PS I, ATP synthase and cytochrome $b_6f$.

## Photosystem II

### *Grana membrane fragments*

The polypeptide pattern of fraction 1 (Figure 2) suggests the presence of PS II core proteins (CP47, CP43, the extrinsic 33 kDa protein or MSP, cytochrome *b*-559) and major and minor LHC II proteins and is virtually the same as that of the 'BBY'-type of PS II membranes prepared according to Berthold et al. (1981) ('B' in Figure 2). The 4 K emission spectrum

*Table 1.* Details of the fractions 1-12 from the gel filtration chromatography (Figure 1). '*t* (min)' represents the average time in minutes after the onset of the chromatography, 'chl *a* / *b*' is the ratio of Chl *a* and *b* determined in 80% acetone using the extinction coefficients reported by Porra et al. (1989), 'cyt*f* (%)' is the relative amount in the various fractions of cytochrome *f* determined from the ascorbate-reduced minus ferricyanide-oxidized absorbance difference spectrum, and '$\lambda_{max}$ (nm)' is the wavelength of the maximum absorption at room temperature in the $Q_y$ absorption region of the chlorophylls

| Fraction | 1 | 2 | 3 | 4 | 5 | 6 | 7 | 8 | 9 | 10 | 11 | 12 |
|---|---|---|---|---|---|---|---|---|---|---|---|---|
| *t* (min) | 17.0 | 18.4 | 19.9 | 21.3 | 22.8 | 24.2 | 25.6 | 27.1 | 28.5 | 30.0 | 31.4 | 32.8 |
| chl *a* / *b* | 2.30 | 2.85 | 4.45 | 6.05 | 7.65 | 8.20 | 6.15 | 2.15 | 1.55 | 1.85 | 2.75 | 3.60 |
| cyt*f* (%) | 2 | 0 | 0 | 0 | 2 | 8 | 37 | 30 | 14 | 5 | 2 | 0 |
| $\lambda_{max}$(nm) | 678.0 | 678.5 | 679.5 | 679.5 | 680.0 | 679.5 | 676.5 | 675.0 | 675.0 | 677.5 | 677.0 | 673.0 |

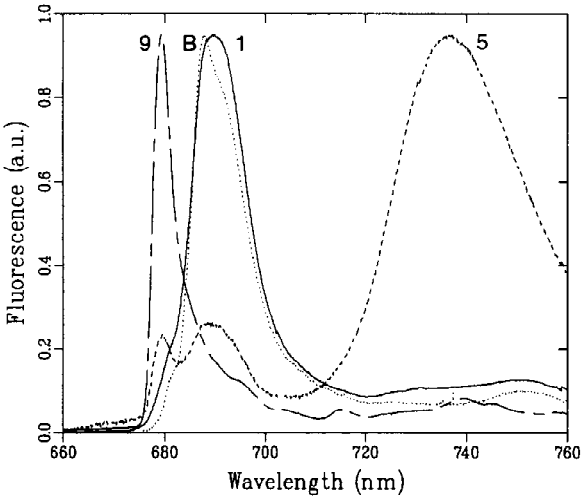


*Figure 4.* 4 K emission spectra of fractions 1 (full line), 5 (dashed line) and 9 (chain-dashed line) from the gel filtration chromatography and of BBY PS II membranes ('B', dotted line), normalized to 1 at the maximum emission value.

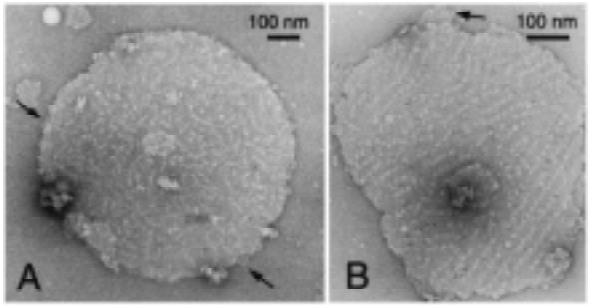


*Figure 5.* Electron micrographs of two exceptionally large inside-out paired grana membrane fragments obtained from fraction 1, negatively stained with 2% uranyl acetate. From the positions of the stain-excluding subunits, which presumably originate from the extrinsic proteins involved in oxygen evolution and which are attached to the core parts of PS II, it can be deduced that the membranes in (A) have a relative low ordering of the PS II core and that those in (B) show a semi-crystalline lattice in which the distance between rows of PS II complexes is about 26.3 nm. The two membranes overlap almost totally, but some small areas which are single layered can be recognized from a different staining pattern (indicated by arrows).

shows a broad band peaking at 690 nm and a shoulder at 680 nm (Figure 4, full line), again similar to that of BBY PS II membranes (Van Dorssen et al. 1987; Figure 4, dotted line). The slightly higher fluorescence yield around 736 nm in fraction 1 compared to the BBY membranes suggests a small contamination with PS I. Also the faint A/B band in the SDS-PAGE pattern of fraction 1 (Figure 2) and the slightly higher Chl *a*/*b* ratio of fraction 1 (2.3 compared to about 2.0 for the BBY membranes) suggest that our preparation still had a small PS I contamination.

The structural organization of PS II and LHC II in fraction 1 was investigated by electron microscopy. Figure 5 shows two electron micrographs which indicate that fraction 1 consists of paired membrane fragments, again similar to the BBY PS II membranes, which were shown to consist of paired, appressed membrane fragments with their lumenal sides exposed (see, e.g., Dunahay et al. 1984; Lyon 1998). In a set of 200 randomly recorded membrane fragments, 68% had a diameter between 300 and 500 nm. The average overall diameter was 360 nm, which is very similar to the value of about 400 nm for membranes in intact grana stacks, as seen in thin sections of spinach chloroplasts (Weibull et al. 1990; Murakami 1991; Olive and Vallon 1991; Staehelin and Van der Staay 1996).

The $\alpha$-DM derived membranes differ, however, in one aspect significantly from the BBY membranes obtained by Triton X-100 treatment. Whereas the latter usually show a total random orientation of their PS II supercomplexes, the $\alpha$-DM derived membranes show a strong degree of two-dimensional ordering, although the amount of semi-crystallinity appears to vary strongly from one membrane to another and

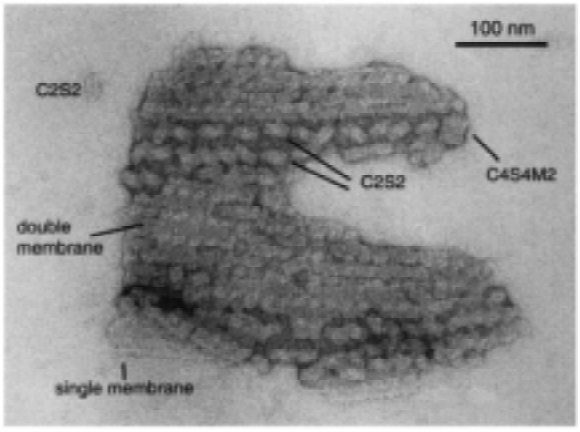


*Figure 6.* Disruption of an average-sized inside-out paired grana membrane fragment obtained from fraction 1 by access of $\alpha$-DM. The central part of the membranes is still consisting of two layers with some periodicity of the PS II supercomplexes whereas the lower left tip is clearly one single layer. Image analysis of the single $C_2S_2$ supercomplexes from the center, which are almost solubilized, indicates that they are all in an upside-down or 'flop' orientation, in which the extrinsic subunits face the carbon support film. In contrast, the freely dispersed molecules laying around this membrane (one supercomplex lacking a CP26 tip is visible in the left upper corner) are in the flip orientation, commonly found by image analysis (Boekema et al. 1999a, b). This indicates that the almost-solubilized $C_2S_2$ complexes are part of the lower membrane.

also within one membrane. The membranes shown in Figures 5A, B represent two extreme examples of variation in this semi-regular ordering. The semi-regular ordering appears as rows at an average distance of about 26.3 nm and resembles the ordering that has been studied more than two decades ago by freeze-fracture electron microscopy (see, e.g., Simpson 1978). An extensive analysis of the semi-regular ordering of PS II in the grana membranes has been recently presented by Boekema et al. (2000).

We conclude that the $\alpha$-DM treatment of the thylakoids results in a selective solubilization of the stromal parts of the membranes and of the interconnecting margins and leaves the appressed granal parts more or less intact. Thus, the $\alpha$-DM treatment gives essentially the same result as the Triton X-100 treatment employed for the preparation of the BBY PS II membranes. We note that, as yet, our $\alpha$-DM treatment can not compete with the Triton X-100 treatment in terms of yield of the PS II membranes and cost effectiveness. However, a very clear advantage is the fact that $\alpha$-DM is a much more gentle detergent for the solubilized fractions than Triton X-100 and allows a detailed analysis of the complexes of the stromal membranes and the margins (see below).

Another advantage of our preparation method is that the grana membranes have been exposed to a small amount of a very mild detergent during a short period of time and that therefore the PS II complexes should be in a relatively native state. Figure 6 shows this unique aspect of the $\alpha$-DM treatment very well. It concerns a membrane fragment of average size which was visualized after treatment with $\alpha$-DM in slight access. Although the two sandwiched membranes are already substantially disrupted, the PS II complexes are still not totally randomnized and the contours of a number of almost solubilized PS II super- and mega-complexes can be easily observed. Most complexes show the characteristic rectangular shape of the most common $C_2S_2$ supercomplex (Boekema et al. 1999a, b). This result gives solid evidence for the idea that this supercomplex represents a basic structural unit of PS II in the grana membranes (see, e.g., Nield et al. 2000).

*Isolated PS II and LHC II complexes*

The intactness of the solubilized complexes from the non-stacked regions of the thylakoid membranes allows an analysis of the amount and properties of the PS II complexes present in the stroma membranes. Biochemical studies have suggested that about 10–15% of the PS II complexes are located in the stroma membranes (reviewed by Lavergne and Briantais 1996) and thus should appear as solubilized complexes in later fractions in our gel filtration chromatogram. Our previous results on PS II complexes prepared from PS II membranes (Boekema et al. 1999a, b) indicate that the various solubilized PS II complexes should be observed somewhere between fraction 4 (dimeric PS II–LHC II supercomplexes) and fraction 7 (monomeric PS II core complexes). Inspection of the gel presented in Figure 2 suggests that the number of 10–15% of PS II complexes in the stroma should be regarded as an upper limit. No significant amount of MSP is observed in these fractions. In addition, EM analysis has shown that dimeric PS II-LHC II supercomplexes are completely absent in fractions 4 and 5 (E.J. Boekema, unpublished observations) and the 4 K emission spectrum of fraction 5 (Figure 4) reveals only a very small amount of PS II fluorescence (most of the emission around 686 nm originates probably from PS I – see below). An immunological analysis of the various fractions will shed more light on this issue.

In contrast to the strongly reduced amounts of PS II core components in the later fractions of the gel filtra-

tion chromatography, it is evident that large amounts of isolated LHC II components have been solubilized. The SDS-PAGE of fractions 8 and 9 clearly shows the presence of the major LHC II proteins (Figure 2), and the absorption (Figure 3) and the fluorescence properties (Figure 4) of fraction 9 are very similar to those of the main trimeric LHC II complex (see, e.g., Hemelrijk et al. 1992). The SDS-PAGE of fractions 10 and 11, in which monomeric LHC complexes are expected, shows a number of other proteins (Figure 2), the most dominant of which co-migrates with CP26. Also the spectroscopic properties of these fractions, such as the higher Chl *a*/*b* ratio and the red shift of the absorption maximum of the chlorophylls (Table 1), suggest the presence of 'minor' monomeric LHC II proteins (see, e.g., Ros et al. 1998; Pascal et al. 1999). It is possible that at a part of this LHC II is involved in the state 1 – state 2 transition and reversibly connects to PS I after phosphorylation (Williams and Allen 1987; Staehelin and Van der Staay 1996).

**Photosystem I**

According to the gel filtration chromatogram and its preliminary analysis (Figure 1) PS I occurs in two main fractions. An analysis of these fractions by electron microscopy and image reconstruction techniques (E.J. Boekema, unpublished observations) has revealed that the smallest complex occurring maximally in fraction 5 can be attributed to monomeric PS I-200 complexes, while the larger complexes occurring predominantly in fraction 3 can be attributed to artificial (upside-up-upside-down) aggregations of these complexes. Also larger aggregates have been observed (trimers, tetramers, etc.).

The SDS-PAGE pattern (Figure 2) shows that the fractions 3–6 are enriched in PS I, although in none of the fractions the PS I complex is pure. In fraction 3 there is a contamination with PS II (most likely some overflow of membrane fragments described above), while the fractions 5 and 6 are heavily contaminated with the $CF_0F_1$ complex. Nevertheless, in all PS I containing fractions not only the large PS I A/B proteins can be observed, but also all four LHC I polypeptides (the bands just above and below the main LHC II band are probably Lhca3 and Lhca2, while the intense band migrating at the same position as CP24 is very likely caused by Lhca1 and Lhca4 – see Jansson et al. 1996) and, below the extrinsic 23K protein of PS II, at least 7 of the small PS I-C/L and PS I-N subunits. The room temperature absorption spectra peak at 679.5–680 nm (Figure 3B, dashed line) and strongly resemble that of the PS I-200 complex in $\beta$-DM (Croce and Bassi 1998). The 4 K emission spectrum (Figure 4, dashed line) shows a broad peak at 736 nm and two much smaller peaks at 679 and 686 nm. A very similar spectrum, including the small peaks at 679 and 686 nm, has been observed for PS I-200 in $\beta$-DM (J. Ihalainen, unpublished observations).

All these results indicate that the $\alpha$-DM treatment leaves the PS I-200 complex intact. Another indication for this is found by a search for isolated LHC I complexes. LHC I is most likely organized as a heterodimer of the Lhca1 and Lhca4 gene products and as a homo- and/or heterodimer of the Lhca2 and Lhca3 gene products (see, e.g., Schmid et al. 1997; Croce and Bassi 1998). This means that LHC I, if present, should be observed predominantly in fraction 10. However, the SDS-PAGE pattern does not reveal the characteristic pattern of the Lhca2, Lhca3 and Lhca1-4 proteins around fraction 10. In addition, as LHC I is expected to display the highest $A_{700}/A_{670}$ ratio of all photosynthetic complexes, its possible presence should be observed as a raise of this ratio around fraction 10, which is not observed (Figure 1, dotted line). A third indication for the absence of free LHC I proteins is found in the 4 K emission spectra, which should show intense bands peaking near 733 and 702 nm (Ihalainen et al. 2000) if intact LHC I is present and which were not observed at all (see the chain-dashed line in Figure 4 for a 4 K emission spectrum of fraction 9). These results indicate that the $\alpha$-DM treatment did not give rise to significant amounts of uncoupled but otherwise intact LHC I complexes. These results clearly differ from those of LHC II (see above). We can not exclude the possibility, however, that small amounts of one or more of the LHC I complexes are present in a monomeric form without long-wavelength chlorophylls. Also in this case a quantitative immunological analysis of the various fractions is required to resolve these questions.

**ATP synthase**

The highest concentration of the $CF_0F_1$ ATP synthase complex is found in fractions 5 and 6. The SDS-PAGE clearly shows the presence of the $\alpha$, $\beta$ and $\gamma$ subunits in these fractions (Figure 2). Electron micrographs of these fractions revealed several hundreds of well-preserved molecular projections of monod-

ispersed ATPase. From 80 negatives of fraction 6 we extracted about 8000 projections for single particle image analysis. In fraction 5 the number of ATPase molecules equalled about the number of PS I-200 molecules. Out of 146 micrographs another 8500 molecules were extracted. A last set of 500 molecules was extracted out of 174 micrographs from fractions 3 and 4, where ATPase is only present in small numbers. The cumulative set of 17 300 projections, which originates from four independent solubilizations, was aligned and treated by multivariate statistics and subsequently classified (see 'Materials and methods'). The last two steps could not be carried out on the complete data set, since the multivariate statistics procedure can not yet handle more than about 10 000 images simultaneously; even on a modern work station the computing of 10 000 images takes already 10 days. The results of both classifications, however, looked rather the same (not shown). Each classification showed three similar groups of classes differing mainly in the overall position of the $F_1$ headpiece relative to $F_0$ (see below). For the final classification step all particles were pooled in one of these 3 groups and re-analyzed. These final results are presented in Figure 7.

The analysis of single particle projection, presented here, is based on the largest number of projections analyzed until now for any F-type or V-type ATPase. Although the resolution, which is about 3 nm, is lower than obtained in the classifications of the related V-type ATPase (Boekema et al. 1999c; Wilkens et al. 1999; Ubbink-Kok et al. 2000), some features were found which have not been observed before.

*Shape and variation of the $F_1$ headpiece*

The high-resolution structure from the ATPase headpiece (Abrahams et al. 1994) shows that the large $\alpha$ and $\beta$ subunits have an overall banana-shaped configuration. The three copies of each of these two subunits are in an hexagonal arrangement and in side-view position in microscopy preparations they show some rotational freedom. This often results in two types of predominant views, in which either two groups of three large subunits overlap ('bilobed views') or three groups of three large subunits overlap ('trilobed views') [see Boekema et al. (1999c) and Ubbink-Kok et al. (2000) for clear examples in the V-type ATPase]. Several classes belong clearly to the trilobed type (15, 21 and 23, Figure 7) or the bilobed type (13, 17, 24, 27). In a previous analysis of about 4700 chloroplast ATPase molecules this feature is harder to see (Böttcher et al. 1998). In some of our classes the tip of the headpiece is quite pointed (12, 15–17, 21, 23, 26–28), but in a few others this tip is absent and instead an indentation is present (20, 22 and 24). This density on top of the headpiece is not present in the X-ray structure from the beef heart enzyme (Abrahams et al. 1994), but was revealed by analysis of about 5000 electron microscopy images of ATPase from the same source (Karrasch and Walker 1999). In the chloroplast ATPase this feature was not very well resolved (Böttcher et al. 1998). Since the $\delta$ subunit (or the equivalent OSCP subunit in mitochondrial ATPase) is known to be somewhere at the top of the headpiece (Engelbrecht and Junge 1997) but absent in the X-ray structure (Abrahams et al. 1994), we interpret the variation in our classes as caused by a partial absence of the $\delta$ subunit. This subunit must for most of its mass be located right on top of the headpiece, in contrast to earlier models where it is placed more at the side (Engelbrecht and Junge 1997; Engelbrecht et al. 1998; Junge et al. 1999), but in agreement with a recent study by Wilkens et al. (2000).

*Shape of the central stalk*

The central stalk of the chloroplast ATPase is formed by the $\epsilon$ subunit and the lower part of the $\gamma$ subunit, as deduced mainly from extensive crosslinking studies (reviewed in Engelbrecht and Junge 1997). In almost all of the classes the central stalk is clearly visible, except for those where the $F_1$ headpiece is closer to $F_0$ than usual (classes 1 and 2, Figure 7). In most of the classes, the central part is clearly the thickest (6–12, 14–16, 18–23) and in some of the classes it appears as an oval density, especially in classes 11 and 18. The crosslinking studies suggest that a major part of the central thick density is formed by the $\epsilon$ subunit. A thicker central part of the central stalk was also observed for beef heart mitochondrial ATPase (Karrasch and Walker 1999), but this enzyme has at least one additional central stalk subunit, which makes a comparison less useful. In contrast, the central stalk region in the classes presented by Böttcher et al. (1998) is somewhat diffuse, without indication for the knobby central density. It could be that this preparation, obtained after extensive purification procedures including 14 hours of ultracentrifugation, had a modified position of $\epsilon$ or some loss of this subunit.

*Presence of the stator*

Despite the fact that we analyzed a very large number

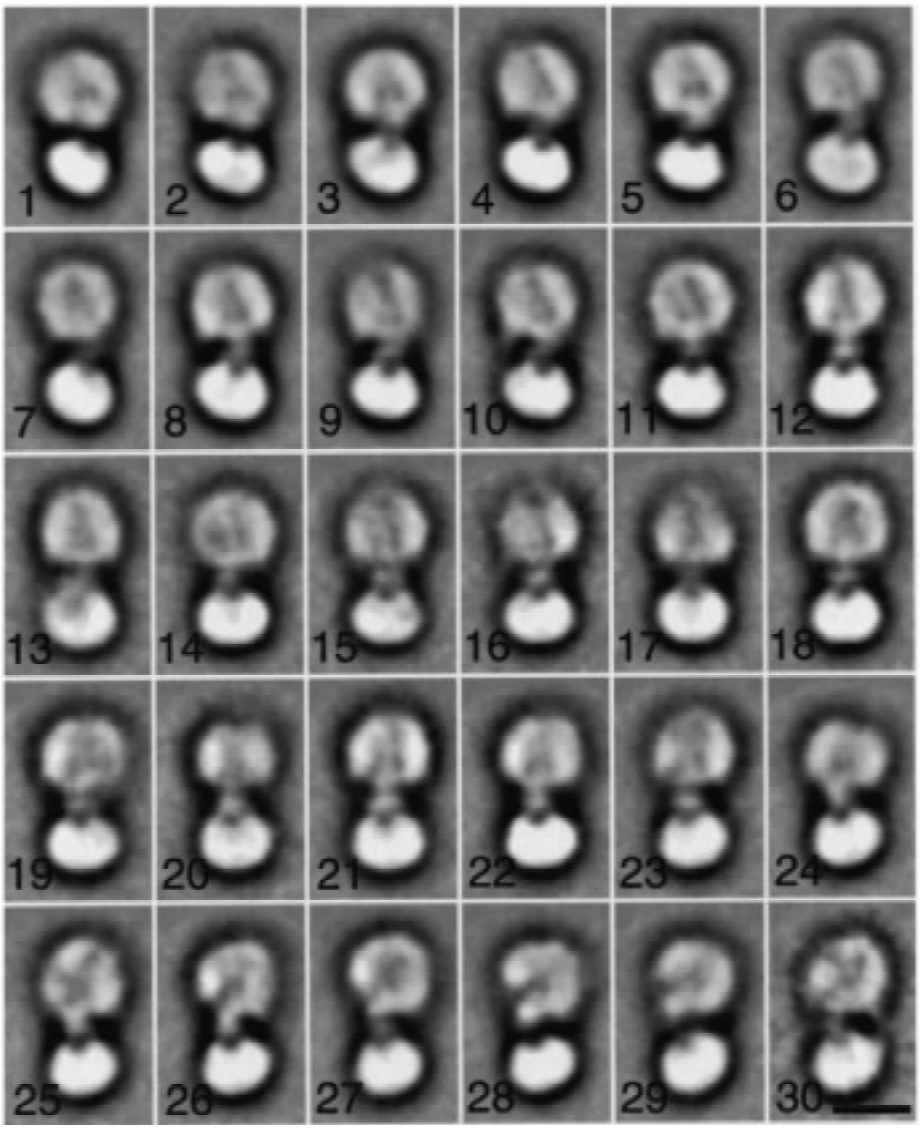


*Figure 7.* Single particle image analysis of a set of 17,300 side-view projections of chloroplast $F_1F_0$ ATPase, obtained mainly from fractions 5 and 6. The first 29 classes (1–29) were derived from three separate classifications. Classes 1–11 represent the best 11 classes out of 12 of particles with the headpiece tilted to the left, classes 12–22 represent the best 11 classes out of 15 with the headpiece in an almost straight position and classes 24–29 represent the best 6 classes out of 10 with the headpiece tilted to the right. Class 30 was obtained from a decomposition of the latter group into 50 classes (instead of 10). Each image is the sum of several hundred projections (except for 30, which is the sum of 65 projections. Bar equals 10 nm.

of particles, the second stalk, or stator, necessary to fix the headpiece to the immobile part of the membrane-bound $F_0$ during rotational catalysis (Noji et al. 1997), is clearly revealed in only a few classes (10, 16, 30), in line with earlier investigations (Böttcher et al. 1999; Karrasch and Walker 1999; Hausrath et al. 1999) where it appeared diffuse as well. Although it could very well be that in some of the classes it is (partly) hidden behind the second stalk (13 and 15?), it is likely that the limited resolution of the classification also plays a role. In the V-type ATPase the stalk region was much better resolved, because it is substantial larger (Boekema et al. 1999c; Wilkens et al. 1999; Ubbink-Kok et al. 2000). This facilitated the observation of one central stalk and two stator structures in the V-type ATPase. In the F-type ATPase there is, however,

no evidence for more than one stator (Boekema et al. 1999c), but it might well be that this stator is totally absent in at least a part of the data set (as it was in the V-type ATPase), especially in those particles which already lack the $\delta$ subunit, as discussed earlier.

*Position of the $F_1$headpiece relative to the $F_0$ part*

The most surprising new feature of our analysis is that a substantial number of molecules show a displacement of the headpiece, either to the left (1–10) or to the right (23–30). The degree of this 'kinking' is somewhat variable over the classes, but quite substantial and almost 90 degrees in the most extreme case (class 30). The bending appears to happen mainly in the stalk, since the structure of the $F_1$headpiece and the membrane-bound $F_0$ part remain largely the same. Kinked molecules were present in about equal numbers in all four independent solubilization experiments from which particles were extracted.

We note that, to our knowledge, similar observations have never been reported. In a recently published ATPase structure of yeast F-type ATPase it can be seen that the central part of $F_0$ (the multimer of the c-subunit, or subunit III in the chloroplast terminology) does not make any significant angle with the base of $F_1$ (Stock et al. 1999) and earlier electron microscopy studies have not indicated any significant displacement of the headpiece as well. Thus, it could well be argued that this novel feature is just an artifact, but there are strong arguments against this reasoning. First comes the very short time of preparation, which was well within an hour, in contrast to, for instance, the procedure of Böttcher and Gräber (1998), which is suspicious of loss of part of the $\epsilon$ subunit. Moreover, it has been shown that during crystallization the yeast ATPase loses several of its subunits from the stalk region and $F_0$ (Stock et al. 1999). Finally, our treatment of the membranes by $\alpha$-DM instead of Triton X-100 can not be regarded as especially harsh. Thus, there are presently no sound arguments to consider the novel finding as an artifact.

This raises the question about its meaning. It is difficult to imagine that the strongly kinked ATPase molecules would still be able to synthesize ATP by rotational catalysis, and since our preparations were prepared in darkness we speculate that the kinked particle projections show the ATPase in its inactive (oxidized) form. The chloroplast ATPase has the unique capacity to undergo large conformational changes upon light-induced activation. These include major rearrangements, especially of the stalk subunits $\gamma$ and $\epsilon$ (Richter and Gao 1996; Hisabori et al. 1998). The rearrangements are not known in detail, but are thought to include a shift in the position of the $\epsilon$ subunit. $\epsilon$ could be more closely associated to $F_1$ in the inactive form and more closely to $F_0$ in the active form (Richter and Gao 1996). As $\epsilon$ moves, it may pull part of the $\gamma$ subunit along with it. Thus, it seems possible that the rearrangements upon activation could also involve a 'straightening' of kinked ATPase headpieces. With our fast isolation procedure we are in a situation to set up *in vitro* experiments with fresh enzyme to investigate if the kinking effect has indeed anything to do with the (in)activation of the chloroplast ATPase at all. It should be stressed again that the $\alpha$-DM method of solubilization is very suitable for this purpose, since a high purity of the stroma components and complete solubilization are not necessary, as long as sufficient single particles can be extracted.

**Cytochrome $b_6f$**

The ascorbate-reduced minus ferricyanide-oxidized absorbance difference spectra of cytochrome *f* (Table 1) clearly indicate that the cytochrome $b_6f$ complex occurred mainly in fractions 7 and 8 and to a minor extent in fraction 9. The presence of an about 34 kDa protein in the SDS-PAGE of fractions 7 and 8 (Figure 2) that can be attributed to cytochrome *f* (see, e.g., Huang et al. 1994) is consistent with these results. The other protein components of the complex are probably present as well, but hard to attribute with certainty because of overlap with similarly-sized proteins from other complexes such as Rubisco (fraction 7) and trimeric LHC II (fraction 8). Based on the position of the cytochrome $b_6f$ complex in the chromatogram we consider it most likely that the complex occurs mainly in a dimeric aggregation state, in agreement with results reported by Huang et al. (1994).

An important issue is the localization of the cytochrome $b_6f$ complex in the thylakoid membranes. It is generally accepted that this complex is not present in the BBY-type of PS II membranes (Berthold et al. 1981), which could mean that this complex is not present in the appressed parts of the grana. However, a number of studies using two-phase aqueous polymer partitioning and immunolabeling or direct immunolabeling have suggested that the cytochrome $b_6f$ complex is more or less evenly distributed between the appressed grana membranes and stroma lamellae

(see, e.g., Allred and Staehelin 1986; Olive et al. 1986; Vallon et al. 1991; Hinshaw and Miller 1993), or that it is even preferentially localized in the grana core vesicles (Albertsson et al. 1991; Albertsson 1995). The absence of the cytochrome $b_6f$ complex from the BBY PS II membranes could then be caused by a selective extraction by the detergent Triton X-100. This is not unreasonable because the BBY procedure involves indeed a rather long incubation step with high concentrations of Triton X-100.

Our results with $\alpha$-DM indicate that a possible detergent-induced removal of the cytochrome $b_6f$ complex from the PS II membranes must have occurred rather quickly and efficiently. With our protocol of preparing PS II membranes, the detergent incubation step takes a very short period of time (a few minutes). This seems very short for an almost complete disappearance of this (large) complex from the stacked membranes. However, in many membranes a number of stain spots were observed (see, e.g., Figure 5B), and it is possible that these spots arise from very local membrane disruptions, caused by the detergent-induced extraction of a membrane-protein complex. The number of spots, however, is much smaller than the number of PS II complexes, and it is therefore unclear if a removal of the cytochrome $b_6f$ complex from the PS II membranes can be responsible for these spots. We note that the spots always occurred randomly, also in those parts of the membrane in which PS II shows a semi-regular organization, and that the organization of PS II in our grana membranes is very similar to that observed before in native chloroplasts that have not been subjected to detergent treatment (discussed above), which is not expected if both membranes would differ by the presence of a large complex as the cytochrome $b_6f$ complex. We conclude from these observations that cytochrome $b_6f$ complex is not present in the semi-regular parts of the grana membranes and that more research is required to fully understand the absence of this complex from our grana membrane fractions.

## Acknowledgements

We thank Dr W. Keegstra for his help with image analysis. Our research was supported in part by the Netherlands Foundation for Scientific Research (NWO) via the Foundation for Life and Earth Sciences (ALW).

## References

Abrahams JP, Leslie AGW, Lutter R and Walker JE (1994) Structure at 2.8 Å resolution of F1-ATPase from bovine heart mitochondria. Nature 370: 621–628

Albertsson P-Å (1995) The structure and function of the chloroplast photosynthetic membrane – a model for the domain organization. Photosynth Res 46: 141–149

Albertsson P-Å, Andreasson E, Svensson P and Yu S-G (1991) Localization of cytochrome *f* in the thylakoid membrane: Evidence for multiple domains. Biochim Biophys Acta 1098: 90–94

Allred DR and Staehelin LA (1986) Spatial organization of the cytochrome $b_6f$ complex within chloroplast thylakoid membranes. Biochim Biophys Acta 849: 94–103

Berthold DA, Babcock GT and Yocum CF (1981) A highly resolved, oxygen-evolving Photosystem II preparation from spinach thylakoid membranes. EPR and electron transport properties. FEBS Lett 134: 231–234

Boekema EJ, van Roon H and Dekker JP (1998) Specific association of Photosystem II and light-harvesting complex II in partially solubilized Photosystem II membranes. FEBS Lett 424: 95–99

Boekema EJ, van Roon H, Calkoen F, Bassi R and Dekker JP (1999a) Multiple types of association of Photosystem II and its light-harvesting antenna in partially solubilized Photosystem II membranes. Biochemistry 38: 2233–2239

Boekema EJ, van Roon H, van Breemen JFL and Dekker JP (1999b) Supramolecular organization of Photosystem II and its light-harvesting antenna in partially solubilized Photosystem II membranes. Eur J Biochem 266: 444–452

Boekema EJ, van Breemen JFL, Brisson A, Ubbink-Kok T, Konings WN and Lolkema JS (1999c) Connecting stalks in V-type ATPase. Nature 401: 37–38

Boekema EJ, van Breemen JFL, van Roon H and Dekker JP (2000) Arrangement of Photosystem II supercomplexes in crystalline macrodomains within the thylakoid membranes of green plants. J Mol Biol 301: 1123–1133

Böttcher B, Schwarz L and Gräber P (1998) Direct indication for the existence of a double stalk in $CF_0F_1$. J Mol Biol 281, 757–762

Croce R and Bassi R (1998) The light-harvesting complex of Photosystem I: Pigment composition and stoichiometry. In: Garab G (ed) Photosynthesis: Mechanisms and Effects, pp 421–424. Kluwer Academic Publishers, Dordrecht, The Netherlands

Dekker JP, van Roon H and Boekema EJ (1999) Heptameric association of light-harvesting complex II trimers in partially solubilized Photosystem II membranes. FEBS Lett 449: 211–214

Dunahay TG, Staehelin LA, Seibert M, Ogilvie PD and Berg SP (1984) Structural, biochemical and biophysical characterization of four oxygen-evolving Photosystem II preparations from spinach. Biochim Biophys Acta 764: 179–193

Eijckelhoff C, van Roon H, Groot M-L, van Grondelle R and Dekker JP (1996) Purification and spectroscopic characterization of Photosystem II reaction center complexes isolated with or without Triton X-100. Biochemistry 35: 12864–12872

Engelbrecht S and Junge W (1997) ATP synthase: A tentative model. FEBS Letters 414: 485–491

Engelbrecht S, Giakas E, Marx O and Junge W (1998) Fluorescence resonance energy transfer mapping of subunit $\delta$ in spinach chloroplast $F_1$ATPase. Eur J Biochem 252: 277–283

Hausrath AC, Grueber G, Matthews BW and Capaldi RA (1999) Structural features of the $\gamma$ subunit of the *Escherichia coli* ATPase revealed by a 4.4-Å resolution map obtained by x-ray crystallography. Proc Natl Acad Sci USA 96: 13697–13702

Hemelrijk PW, Kwa SLS, van Grondelle R and Dekker JP (1992) Spectroscopic properties of LHC-II, the main light-harvesting

chlorophyll *a/b* protein complex from chloroplast membranes. Biochim Biophys Acta 1098: 159–166

Hinshaw J and Miller KR (1993) Mapping the lateral distribution of Photosystem II and the Cytochrome $b_6/f$ complex by direct immune labeling of the thylakoid membrane. J Struct Biol 111: 1–8

Hisabori T, Motohashi K, Kroth P, Strotmann H and Amano T (1998) The formation or the reduction of a disulfide bridge on the $\gamma$ subunit of the chloroplast ATP synthase affects the inhibitory effect of the $\epsilon$ subunit. J Biol Chem 25: 15901–15905

Huang D, Everly RM, Cheng RH, Heymann JB, Schägger H, Sled V, Ohnishi T, Baker TS and Cramer WA (1994) Characterization of the chloroplast cytochrome $b_6f$ complex as a structural and functional dimer. Biochemistry 33: 4401–4409

Ihalainen JA, Gobets B, Sznee K, Brazzoli M, Croce R, Bassi R, van Grondelle R, Korppi-Tommola JEI and Dekker JP (2000) Evidence for two spectroscopically different dimers of light-harvesting complex I from green plants. Biochemistry 39: 8625–8631

Jansson S, Andersen B and Scheller HV (1996) Nearest-neighbor analysis of higher-plant Photosystem I holocomplex. Plant Physiol 112: 409–420

Junge W (1999) ATP synthase and other motor proteins. Proc Natl Acad Sci USA 96: 4735–4737

Karrasch S and Walker JE (1999) Novel features in the structure of bovine ATP synthase. J Mol Biol 290: 379–384

Kühlbrandt W, Wang DN and Fujiyoshi Y (1994) Atomic model of plant light-harvesting complex by electron crystallography. Nature 367: 614–621

Lavergne J and Briantais J-M (1996) Photosystem II heterogeneity. In: Ort DR and Yocum CF (eds) Oxygenic Photosynthesis: The Light Reactions, pp 263–287. Kluwer Academic Publishers, Dordrecht, The Netherlands

Lyon MK (1998) Multiple crystal types reveal Photosystem II to be a dimer. Biochim Biophys Acta 1364: 403–419

Murakami S (1991) Structural and functional organization of the thylakoid membrane system in photosynthetic apparatus. J Electr Microsc 41: 424–433

Nield J, Orlova EV, Morris EP, Gowen B, van Heel M and Barber J (2000) 3D map of the plant Photosystem II supercomplex obtained by cryoelectron microscopy and single particle analysis. Nature Struct Biol 7, 44–47

Noji H, Yasuda R, Yoshida M, Kinosita K (1997) Direct observation of the rotation of $F_1$-ATPase. Nature 386: 299–302

Olive J and Vallon O (1991) Structural organization of the thylakoid membrane: freeze-fracture and immunocytochemical analysis. J Electron Microsc Technique 18: 360–374

Olive J, Vallon O, Wollman F-A, Recouvreur M and Bennoun P (1986) Studies of the cytochrome $b_6/f$ complex. II. Localization of the complex in the thylakoid membranes from spinach and *Chlamydomonas reinhardtii* by immunocytochemistry and freeze-fracture analysis of $b_6/f$ mutants. Biochim Biophys Acta 851: 239–248

Pascal AA, Gradinaru CC, Wacker U, Peterman EJG, Calkoen F, Irrgang K-D, Horton P, Renger G, van Grondelle R, Robert B and van Amerongen H (1999) Spectroscopic characterization of the spinach Lhcb4 protein (CP29), a minor light-harvesting complex of Photosystem II. Eur J Biochem 262: 817–823

Porra RJ, Thompson WA and Kriedemann PE (1989) Determination of accurate extinction coefficients and simultaneous equations for assaying chlorophyll-a and chlorophyll-b extracted with 4 different solvents – verification of the concentration of chlorophyll standards by atomic-absorption spectroscopy. Biochim Biophys Acta 975: 374–384

Rhee K-H, Morris EP, Barber J and Kühlbrandt W (1998) Three-dimensional structure of the plant Photosystem II reaction centre at 8 Å resolution. Nature 396: 283–286

Richter ML and Gao F (1996) The chloroplast ATP synthase: structural changes during catalysis. J Bioenerg Biomembr 28: 443–449

Ros F, Bassi R and Paulsen H (1998) Pigment-binding properties of the recombinant Photosystem II subunit CP26 reconstituted *in vitro*. Eur J Biochem 253: 653–658

Schägger H and von Jagow G (1987) Tricine-sodium dodecyl sulfate-polyacrylamide gel electrophoresis for the separation of proteins in the range from 1 to 100 kDa. Anal Biochem 166: 368–379

Schmid VHR, Cammarata KV, Bruns BU and Schmidt GW (1997) *In vitro* reconstitution of the Photosystem I light-harvesting complex LHC I-730. Heterodimerization is required for antenna pigment organization. Proc Natl Acad Sci USA 94: 7667–7672

Schubert W-D, Klukas O, Krauss N, Saenger W, Fromme P and Witt HT (1997) Photosystem I of *Synechococcus elongatus* at 4 Å resolution: Comprehensive structure analysis. J Mol Biol 272: 741–769

Simpson DJ (1978) Freeze-fracture studies on barley plastid membranes. II. Wild-type chloroplasts. Carlsberg Res Commun 43: 365–389

Staehelin LA and van der Staay GWM (1996) Structure, composition, functional organization and dynamic properties of thylakoid membranes. In Ort DR and Yocum CF (eds) Oxygenic Photosynthesis: The Light Reactions, pp 11–30. Kluwer Academic Publishers, Dordrecht, The Netherlands

Stock D, Leslie AGW and Walker JE (1999) Molecular architecture of the rotary motor in ATP synthase. Science 286: 1700–1705

Ubbink-Kok T, Boekema EJ, van Breemen JFL, Brisson A, Konings WN and Lolkema JS (2000) Stator structure and subunit composition of the $V_1/V_0$ $Na^+$-ATPase of the thermophilic bacterium *Caloramator fervidus*. J Mol Biol 296: 311–321

Vallon O, Bulte L, Dainese P, Olive J, Bassi R and Wollman FA (1991) Lateral redistribution of cytochrome $b_6/f$ complexes along thylakoid membranes upon state transitions. Proc Natl Acad Sci USA 88: 8262–8266

Van Dorssen RJ, Plijter JJ, Dekker JP, den Ouden A, Amesz J and van Gorkom HJ (1987) Spectroscopic properties of chloroplast grana membranes and of the core of Photosystem II. Biochim Biophys Acta 890: 134–143

Van Heel M (1989) Classification of very large electron microscopical image data sets. Optik 82: 114–126

Van Heel M and Frank J (1981) Use of multivariate statistics in analysing images of biological macromolecules. Ultramicroscopy 6: 187–194

Weibull C, Villiger W and Bohrmann B (1990) Ultrastructure of spinach chloroplasts as revealed by freeze-substitution. J Struct Biol 104: 139–143

Wilkens S, Vasilyeva E and Forgac M (1999) Structure of the vacuolar ATPase by electron microscopy. J Biol Chem 274: 31804–31810

Wilkens S, Zhou J, Nakayama R, Dunn SD and Capaldi RA (2000) Localization of the delta subunit in the *Escherichia coli* F1F0-ATPsynthase by immune electron microscopy: The subunit delta binds on top of the F-1. J Mol Biol 295: 387–391

Williams WP and Allen JF (1987) State 1-state 2 changes in higher plants and algae. Photosynth Res 13: 19–45